Defective development of photoreceptor membranes in a mouse model of recessive retinal degeneration

Alecia K. Gross *, Glenn Decker, Fung Chan, Ivette M. Sandoval,
John H. Wilson, Theodore G. Wensel

Verna and Marrs McLean Department of Biochemistry and Molecular Biology, Baylor College of Medicine, Houston, TX 77030, USA

Abstract

Retinal neurodegeneration occurs in several inherited diseases. Some of the most severe disease alleles involve mutations at the C-terminus of rhodopsin, but in no case is the pathogenic mechanism leading to cell death well understood. We have examined a mouse model of recessive retinal degeneration caused by a knock-in of a human rhodopsin-EGFP fusion gene (*hrhoG/hrhoG*) at the rhodopsin locus. Whereas heterozygous mutant mice were indistinguishable from control mice, homozygous mutant mice had retinal degeneration. We hypothesized that degeneration might be due to aberrant rhodopsin signaling; however, inhibiting signaling by rearing mice in total darkness had no effect on the rate of degeneration. Using confocal and electron microscopy, we identified the fundamental defect as failed biogenesis of disk membranes, which is observed at the earliest stages of outer segment development. These results reveal that in addition to its role in transport and sorting of rhodopsin to disk membranes, rhodopsin is also essential for formation of disks.
© 2006 Elsevier Ltd. All rights reserved.

Keywords: Retinal degeneration; Rhodopsin; Photoreceptor; Membrane biogenesis; Electron microscopy (EM)

1. Introduction

Proper sorting and targeting of membrane proteins and lipids are critical in generating and maintaining the membrane asymmetry of polarized neuronal and epithelial cells. Although establishing and maintaining proper membrane structures and compositions in distinct compartments is especially important for rod photoreceptor cells, the process is not fully understood. Rods are distinctly polarized ciliary neurons containing light-sensing outer segments (OSs)[1] and distal synaptic termini, separated by an inner segment occupied by the nucleus and membranous organelles. The rod outer segment (ROS), filled with a series of flattened sacks of membranes known as disks, is linked to the inner segment via a connecting cilium that contains a 9-plus-zero bundle of microtubules encased in a sheath of plasma membrane and a thin layer of cytoplasm. The protein composition of the disk membranes is completely different from that of the inner segment plasma membrane. The disk membranes include roughly equal masses of lipid and rhodopsin, the G-protein coupled receptor responsible for capturing photons of light and initiating the phototransduction cycle. Whereas rhodopsin is present at a formal concentration of 3 mM in the outer segments, it is barely detectable in the inner segments of healthy rods.

The synthesis of rhodopsin and assembly of disk membranes occur at a rapid pace throughout the life of a rod cell. Daily, the distal tips of ROSs are phagocytosed by neighboring retinal pigmented epithelium cells, and new disks are formed at the interface of the connecting cilium and the outer segment region, necessitating continual replacement by newly assembled disk membranes. Membrane protein synthesis is confined to the rough endoplasmic reticulum of the inner segment and the newly

---

synthesized proteins traverse the connecting cilium between the inner and outer segments to form the disks of the ROS. Maintenance of organization throughout the cycle of ROS renewal is crucial for the health of photoreceptor cells.

Photoreceptor health is critical for structural and functional maintenance of vertebrate retina. Several retinal degenerative diseases are caused by mutations in the rhodopsin gene that have been proposed to lead to defective rhodopsin sorting to disk membranes (Deretic, Schmerl, Hargrave, Arendt, & McDowell, 1998; Deretic et al., 2005; Tam, Moritz, Hurd, & Papermaster, 2000). Degeneration typically begins with rod cell death, followed by cone cell death and eventually by death of higher order neurons, but the pathophysiology leading from rhodopsin mutations to rod cell death is still not well understood.

Mice homozygous for a knock-in of a human rhodopsin-EGFP fusion gene (*hrhoG/hrhoG*) at the mouse rhodopsin locus suffer from progressive retinal degeneration, whereas heterozygous mice (+/*hrhoG*) do not (Chan, Bradley, Wensel, & Wilson, 2004). We have used laser scanning confocal fluorescence microscopy and transmission electron microscopy to determine the effects of the modified rhodopsin on membrane structure, at different stages of outer segment development. We have also compared the progress of degeneration in mice raised in normal light/dark cycles or in complete darkness to assess the role of rhodopsin-GFP photoactivation in the degeneration.

2. Methods

2.1. Confocal fluorescence microscopy

Eyes were collected from euthanized mice, fixed in 4% paraformaldehyde in phosphate buffered saline (PBS, pH 7.3) for 1 h at room temperature with gentle rotation, followed by 1 h in 30% sucrose in PBS, pH 7.3. The eyes were frozen on dry ice in 100% Tissue-Tek O.C.T. compound (Sakura Finetek USA, Torrance, CA) and sliced in 12 μm thin sections with a Microm HM 500 microtome (Microm Instruments, Heidelberg, Germany.) The slices were air-dried, washed three times in PBS at room temperature for 30 min each. Images were captured after mounting with Gel/Mount (Biomeda, Foster City, CA) on an Olympus Fluoview 300 confocal scanning system interfaced to an IX-70 microscope with a 60×, 1.42 n.a. oil immersion objective. To obtain sub-saturated images, photomultiplier tube voltages were adjusted so that only the brightest few pixels in the brightest image in a series had the highest signal level (4095). For saturated images, voltages were adjusted to allow visualization of the entire photoreceptor layer.

Images were captured from various locations in the retina, excluding areas around the optic nerve and the periphery. Confocal images were used to count nuclei in the outer nuclear layer. We counted 30–100 columns of nuclei for each retina and averaged them for each time point.

2.2. Transmission electron microscopy

Mouse eyecups were fixed by immersion in 2.5% paraformaldehyde, 2.5% glutaraldehyde in 100 mM sodium cacodylate buffer, pH 7.4, at room temperature for 30 min, then at 4 °C for 2 h with gentle rotation. The eyecups were then washed with 60 mM sodium phosphate, pH 7.4, supplemented with 3% sucrose, 150 mM $CaCl_2$ two times, 15 min each, then secondarily fixed with 1% OsO_4 in 60 mM sodium phosphate, pH 7.4 supplemented with 3% sucrose and 150 mM $CaCl_2$. The eyecups were dehydrated through an ethanol series and transitioned to the embedding

medium with propylene oxide. The eyecups were embedded for sectioning in 29% (w/w) Araldite 502, 17.8% (w/w) LX-112, 53.2% (w/w) dodecenyl succinic anhydride (DDSA) supplemented with 0.2 ml benzyldimethylamine (BDMA)/ 10 g resin at 70 °C for 8 h. All reagents were from Electron Microscopy Sciences, Hatfield, PA (USA). Ultrathin sections (80 nm) were cut from the samples using a RMC MT6000 ultramicrotome, mounted on 100-mesh grids, stained with 2% alcoholic uranyl acetate and Reynold's lead citrate. Grids were examined and photographed in a transmission electron microscope (Zeiss EM 902). The micrograph negatives were digitized by scanning to a Dell computer with a Nikon Super Coolscan 9000 ED. Intensity and size of images were adjusted using Adobe Photoshop CS (version 8.0). Images were taken from two to four animals at each age.

2.3. Dark rearing

For dark rearing studies, mice were housed in a dark room in accordance with approved animal use protocols. Animal husbandry was performed with the aid of ON 1 × 20 military night vision goggles (Night Vision Optics Dot Com, Washougal, WA). For light–dark rearing studies, lights were set to a standard 14-h light cycle with lights on from 8 a.m. and off at 8.p.m.

3. Results

3.1. Retinal degeneration in rhodopsin-GFP knock-in mice

Mice heterozygous for rhodopsin-GFP maintain healthy retinas for up to a year (Chan et al., 2004), as shown by fluorescent confocal images of retinal cryosections (Fig. 1). Images at saturating intensities (Fig. 1, column 1) amplify trace amounts of rhodopsin-GFP throughout rod cells, revealing a well-organized outer nuclear layer. In sub-saturated images (Fig. 1, column 2), fluorescence is confined to the ROSs, which show uniform green fluorescence throughout their entire length. Moreover, there is a clear line of demarcation between the outer and inner segment regions. These results indicate that despite the presence of a 26-kDa protein fused adjacent to the C-terminal sorting sequence (Chuang & Sung, 1998; Deretic et al., 1998) of rhodopsin, rhodopsin-GFP is efficiently exported to the outer segment and excluded from the inner segment, as is wild-type rhodopsin.

In contrast, homozygous mice undergo progressive retinal degeneration (Fig. 1, column 3). The thickness of the retinal layer decreases with time as photoreceptors die. By 10 weeks postnatal, only a few nuclei remain in the outer nuclear layer, and no more than one nucleus is observed in any row at 14 weeks. In homozygotes, the outer segment morphology is abnormal at all ages, with nascent rod outer segments showing non-uniform clumps of fluorescence as early as 2 weeks. In addition, the outer and inner segment boundaries are difficult to distinguish, and there are heterogeneous patches of green fluorescence adjacent to the outer nuclear layer. The distribution of rhodopsin-GFP in homozygotes differs from that in the heterozygotes: greater fluorescence was observed in the distal outer segments than in the proximal part of the outer segments. As the retinal degeneration progresses, rhodopsin-GFP continues to be concentrated at the distal ends of the remaining cells where
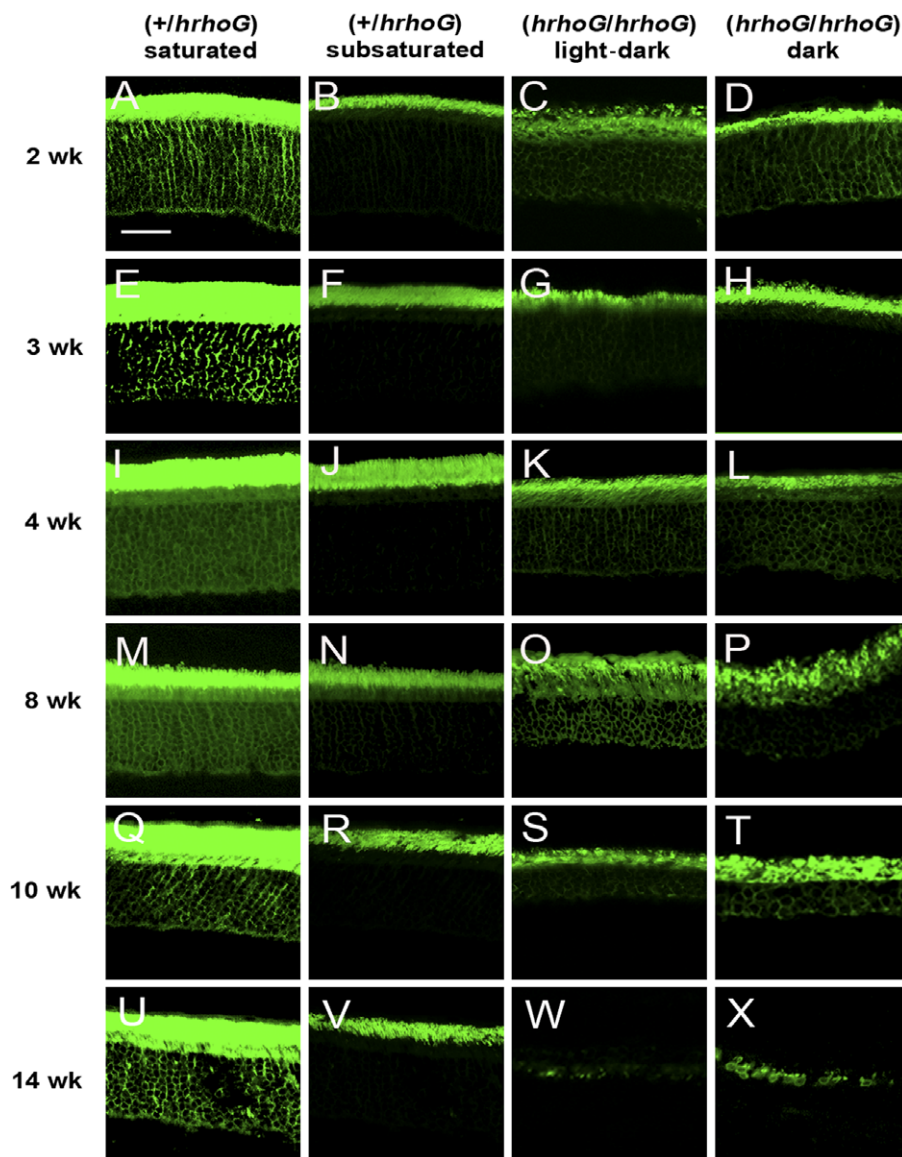
Fig. 1. Confocal fluorescence images of retinal sections from mice expressing human rhodopsin-GFP. The first column (A, E, I, M, Q, and U) shows retinal sections from 2- to 14-week-old heterozygous mice raised in standard light cycles, with the fluorescence signal amplified to show the outer nuclear layer. The second column (B, F, J, N, R, and V) shows the same sections from heterozygous mice raised in normal light cycles at sub-saturating signal intensities. The third (C, G, K, O, S, and W) and fourth (D, H, L, P, T, and X) columns show sections at sub-saturating intensities from 2- to 14-week-old old homozygous mice raised in normal light cycles (third column, C, G, K, O, S, and W) or raised in total darkness (fourth column, D, H, L, P, T, and X).

brightly fluorescent remnants of outer segments can be seen. Even at the resolution of confocal microscopy, the outer segments have abnormal morphology (Fig. 1, column 3).

3.2. Retinal degeneration in dark-reared mice

To determine whether rhodopsin signaling is involved in the mechanism of degeneration in homozygotes, we compared mice that were reared in darkness with those that were reared in a standard light/dark cycle. Retinal sections from homozygotes reared in total darkness were inspected by laser-scanning confocal fluorescence microscopy for retinal degeneration (Fig. 1, column 4). Comparison of age-matched retinas from light/dark-reared and dark-reared homozygous mice show no appreciable differences.

Quantification of retinal degeneration by counting the number of nuclei in the outer nuclear layer shows that the rates of degeneration are identical in light/dark and dark-reared mice (Fig. 2). The absence of a dependence on light suggests that photoresponse defects, if they exist, are not fundamental to the mechanism of degeneration.

3.3. Ultrastructure of rod photoreceptors

To follow the ultrastructural changes accompanying degeneration and cell death, we imaged the retina by transmission electron microscopy. Low magnification images of retinas from wild-type animals (+/+) at all ages show outer segment, inner segment, and outer nuclear layers with distinct boundaries between each layer (Fig. 3A–D). At higher
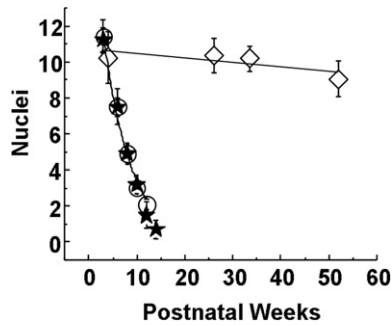
Fig. 2. Loss of photoreceptors in outer nuclear layer. Nuclei in 30–100 individual rows in the outer nuclear layers of retinal sections from wild type and hrhoG/hrhoG at indicated ages were counted and averaged. Diamonds, +/+; circles, hrhoG/hrhoG raised in normal light/dark cycles; filled stars, hrhoG/hrhoG raised in total darkness.

magnification the outer segments at all ages display the stacked disk structure typical of rod outer segments (Fig. 3E–H). The ultrastructure of the photoreceptors in heterozygotes (+/hrhoG) is indistinguishable from that of wild-type retina (Fig. 4). In retinas from both wild type and heterozygous mice the lengths of the rod outer segments are similar, as are the lengths of the inner segments, and the stacked disks are uniformly spaced and well aligned with the plasma membrane. In contrast, the ultrastructure of retinas from homozygous mice (hrhoG/hrhoG) reared under standard light/dark cycles is aberrant even at 3 weeks of age, when little cell death has occurred (Fig. 5A and E). At 3, 6, and 8 weeks postnatal the boundary between the inner and outer segments is indistinct (Fig. 5A–C) in contrast to the well-defined boundaries observed in retinas from +/+ and +/hrhoG mice (Figs. 3 and 4). Moreover, even before there has been significant loss of nuclei, disordered swirls of membrane, as well as disk stacks with wider spacing than normal and dispersed areas of disorder, are visible in the rod outer segments (Fig. 5E–G). These same ultrastructural

abnormalities are present in dark-reared mice, as well (data not shown).

3.4. Biogenesis of rod outer segment membrane

Rhodopsin expression is first detectable 5 days after birth and rod outer segments begin to form shortly thereafter (Bibb et al., 2001). To examine the effects on the biogenesis of the characteristic stacked disk structure of rod outer segments, we examined retinal ultrastructure at 10 and 28 days postnatal. In Fig. 6 we show the ultrastructure of rod cells in wild-type mice (+/+; 100% rhodopsin), homozygous knockout mice (−/−; 0% rhodopsin) (Humphries et al., 1997), homozygous knock-in mice (hrhoG/hrhoG; 80% rhodopsin-GFP), knock-in mice generated by segmental replacement (hrhoG(H)/hrhoG(H); 16% rhodopsin-GFP), (Chan et al., 2004) and heterozygous knock-in mice (+/hrhoG; 50% rhodopsin, 40% rhodopsin-GFP). These results are in Table 1.

Comparisons of rod ultrastructure in these mice allow us to draw several conclusions. First, the initial formation of rod outer segments in wild type and heterozygous (+/hrhoG) mice (Fig. 6A and C) is indistinguishable, indicating that rhodopsin-GFP, present at 80% the level of wild-type rhodopsin, does not interfere with the formation of rod outer segments. The disorganized lamellae visible in the early stages of outer segment formation (10 days) in both wild type and heterozygous mice are ultimately replaced with the well-ordered disks characteristic of rod outer segments (Fig. 6B and D). Second, in the absence of wild type rhodopsin, rods expressing rhodopsin-GFP at 80% (hrhoG/hrhoG) or 16% (hrhoG(H)/hrhoG(H)) of normal levels have readily apparent defects in initial formation of rod outer segments (Fig. 6E and G) that do not resolve into a standard array of disks (Fig. 6F and H). The amount of lamellar disk-like material is greater in hrhoG
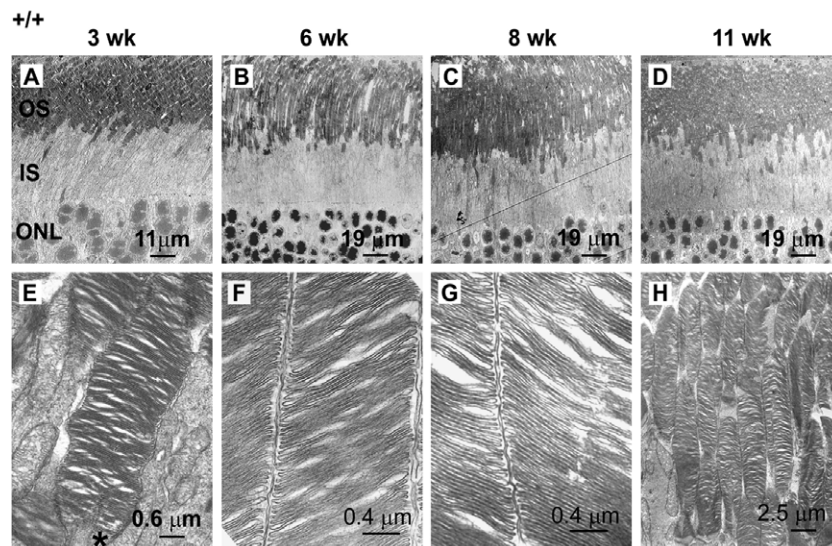

Fig. 3. Electron micrographs of retinas from wild-type mice. Ultrathin sections of retinas taken from mice of various ages were examined by electron microscopy. Low magnification images (A–D) show delineation of outer segment (OS), inner segment (IS), and outer nuclear layer (ONL) areas. High magnification images (E–H) show the stacked disks of the outer segments. A connecting cilium (∗) is visible in E. Scale bars are indicated.
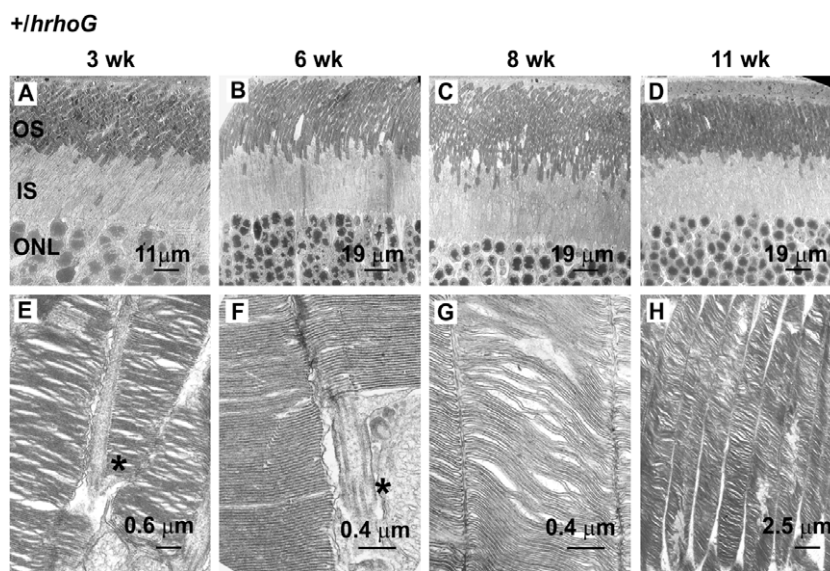
Fig. 4. Electron micrographs of retinas from heterozygous (+/hrhoG) mice. Ultrathin sections of retinas from mice of various ages were examined by electron microscopy. Low magnification images (A–D) show the organization of the outer (OS) and inner segments (IS) and of the outer nuclear layer (ONL). High magnification images (E–H) show the stacked discs of the rod outer segments. Connecting cilia (∗) can be seen in E and F. Scale bars are indicated.
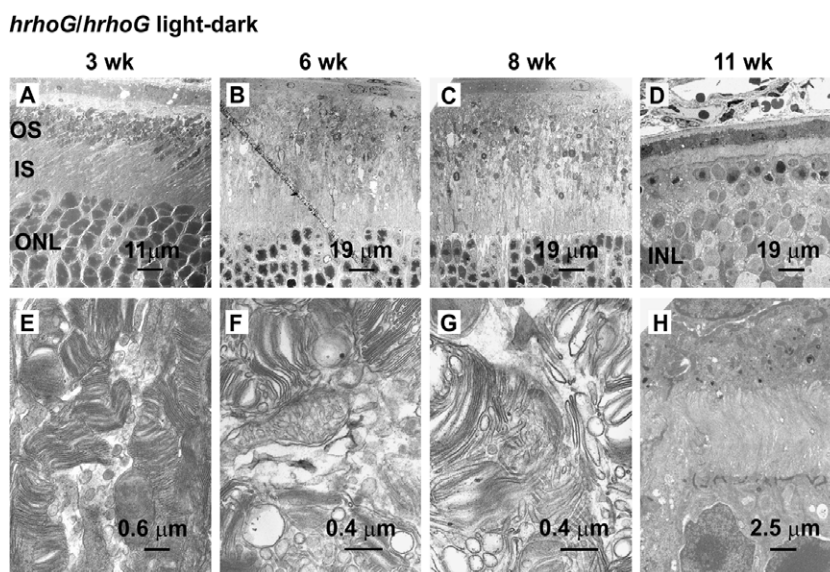

Fig. 5. Electron micrographs of retinas from homozygous (hrhoG/hrhoG) mice. Ultrathin sections of retinas from mice of various ages were examined by electron microscopy. Low magnification images (A–D) show the organization of the outer (OS) and inner segment (IS) and of the outer nuclear layer (ONL). At age 11 weeks, outer segments and inner segments are no longer visible (D). High magnification images (E–G) show the severely disorganized outer segment membranes present at ages 3, 6, and 8 weeks. No disk-like membranes are detectable at age 11 weeks (H). Scale bars are indicated.

homozygotes than in hrhoG(H) homozygotes, suggesting that rhodopsin-GFP contributes to disk formation, although it does not prevent retinal degeneration. Finally, there are similarities in membrane disorganization in mice lacking wild-type rhodopsin whether rhodopsin-GFP is present or not (Fig. 6E,G, and I).

4. Discussion

Several animal models of dominant mutations in rhodopsin leading to retinal degeneration have been described (http://eyegene.meei.harvard.edu/, Schuster et al., 2005; Wilson & Wensel, 2003) and a few human recessive mutations in rhodopsin have been characterized (Fujiki et al., 1995; Rosenfeld et al., 1992). Previously, the only animal model for recessive retinitis pigmentosa was the rhodopsin null allele (Humphries et al., 1997). The mouse models presented here, which maintain normal retinal morphology in the heterozygote, but undergo fairly rapid degeneration in the homozygote, present an opportunity for exploring the underlying causes of recessive retinal degeneration.
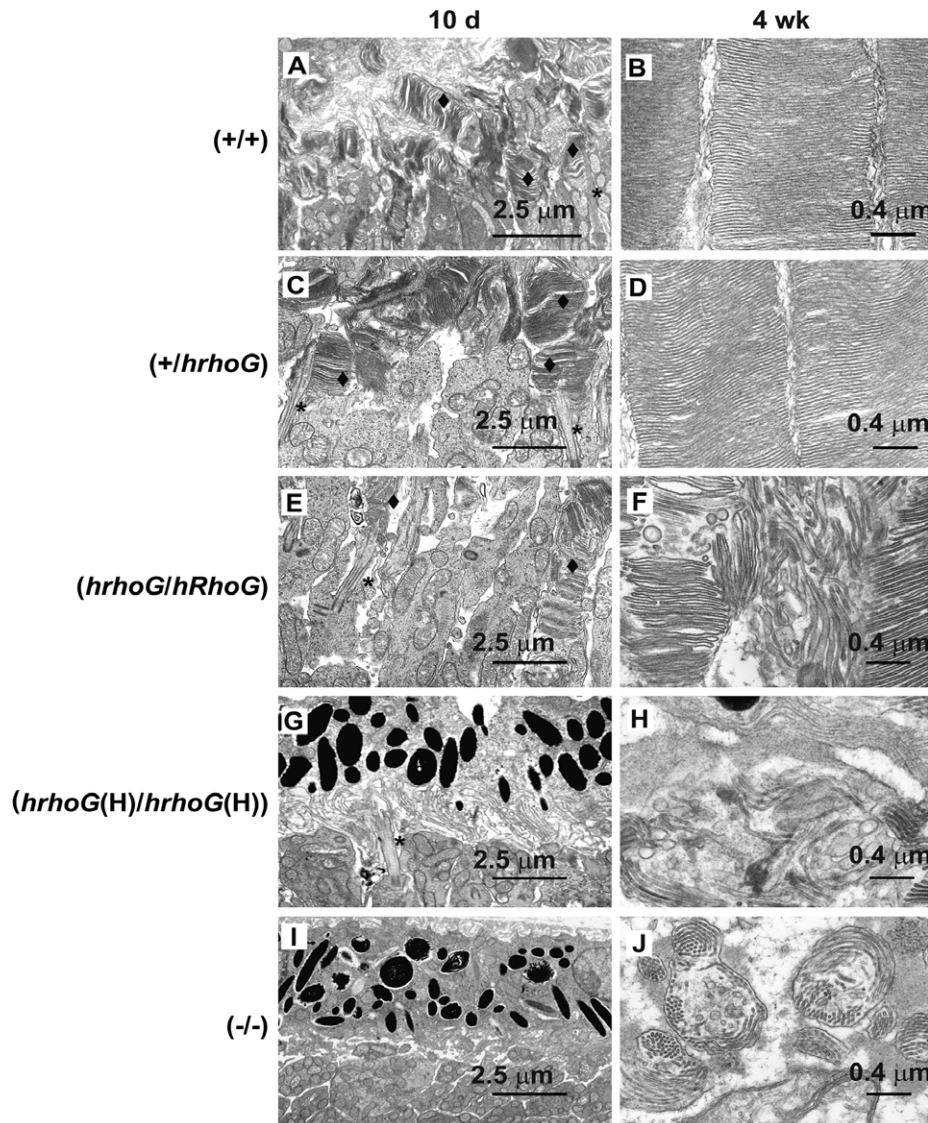
Fig. 6. Electron micrographs of retinas from mice of various genotypes at early stages of development. Ultrathin sections of retinas from various mice at 10 and 28 days postnatal were examined by electron microscopy. A and B, +/+ mouse eye; C and D, +/hrhoG mouse eye; E and F, hrhoG/hrhoG mouse eye; G and H, hrhoG(H)/hrhoG(H) mouse eye; I and J, −/− mouse eye. Scale bars are indicated. Connecting cilia (asterisks) are visible in A, C, E, and G. Diamonds indicate growing disk stacks in wild type (+/+) and heterozygous (+/hrhoG) mice (A and C) and disorganized lamellae in homozygous (hrhoG/hrhoG) mice (E). Dark areas in G and I are pigment granules in the retinal pigmented epithelium.

In designing the experiments reported here, we considered three hypotheses as possible explanations for cell death observed in mice homozygous for rhodopsin-GFP alleles: (1) hyper-sensitivity to light-induced damage associated with aberrant signaling by rhodopsin-GFP; (2) concentration-dependent toxicity of rhodopsin-GFP not associated with light-induced signaling; (3) lack of an essential function fulfilled by wild-type rhodopsin but not by rhodopsin-GFP.

Photoreceptor cell death can be induced by exposure to light, and the amount of damage can vary according to a variety of factors including duration of light, intensity, previous history of light exposure, genetic background of animal, and age. Mice deficient in phototransduction regulatory genes, arrestin, and rhodopsin kinase, are highly sensitive to light exposure (Chen, Burns et al., 1999; Chen, Simon, Matthes, Yasumura, & La Vail, 1999; Choi, Hao, Chen, & Simon, 2001). These mice have normal retinal morphology when raised in the dark, but when exposed to continuous light, they have a rapid induction of photoreceptor apoptosis.

The identical rates of retinal degeneration in light/dark cycle-reared and constant dark-reared mice argue strongly against the hypothesis that a perturbation of light-dependent signaling by rhodopsin-GFP causes the degeneration. This conclusion is supported by the identical morphological defects in light/dark and dark-reared mice as observed at both the fluorescence and electron microscopy levels, and by the identical rates of cell death. These results are in contrast to degenerative conditions involving mutations in phototransduction proteins, such as rhodopsin knockout and arrestin knockout mice, in which degeneration is light-dependent.

Table 1
Summary of rhodopsin expression, retinal degeneration, and outer segment membrane structure in various mouse genotypes

Genotype	Mouse rhodopsin (%)	Human rhodopsin-GFP (%)	Degeneration[a] (half-life[b])	Rod outer segment membranes
+/+	100	0	No (299)[c]	Normal
+/−	50	0	No (approx. 39)[d]	Normal[d]
−/−	0	0	Yes (3.8)[d]	Grossly disrupted
hrhoG/hrhoG	0	80	Yes (3.9)[c]	Disorganized
+/*hrhoG*	50	40	No (42)[c]	Normal
hrhoG(H)/*hrhoG*(H)	0	16	Yes (6.6)[c]	Disorganized
+/*hrhoG*(H)	50	8	No (106)[c]	ND[c]

[a] Defined as loss of more than half of nuclei within six months.
[b] Weeks.
[c] Chan et al., 2004.
[d] Humphries et al. (1997).

An "equivalent light" hypothesis has been proposed that suggests a link between retinal degeneration due to light damage and degeneration due to excessive signaling as a result of defects in proteins, such as RPE65, that regulate rhodopsin function (Fain & Lisman, 1993; Fain & Lisman, 1999; Lisman & Fain, 1995). Clearly this class of mechanisms cannot account for the effects of the recessive alleles studied here.

The second hypothesis, a toxic effect of excessive levels of rhodopsin-GFP, is suggested by the recessive nature of the disease and by observation of GFP toxicity in other systems. For example, virus-directed overexpression of GFP is toxic to dopamine neurons in the brain (Klein et al., 2006). The strongest argument against such a toxic effect in the mice described here comes from comparing results with +/*hrhoG* mice to those with *hrhoG*(H)/*hrhoG*(H) mice. The knock-in mice generated by segmental replacement, *hrhoG*(H)/*hrhoG*(H), have only 40% as much rhodopsin-GFP as heterozygous +/*hrhoG* mice, yet they undergo a much more rapid course of degeneration and photoreceptor cell death (Chan et al., 2004) (Table 1). The retinas of the *hrhoG*(H)/*hrhoG*(H) and the rhodopsin null (−/−) mice both have very low concentrations of the rhodopsin protein (Table 1). Tightly curved and closely packed membranes still occur in both of these genotypes (Fig. 6G and I) (Lee, Burnside, & Flannery, 2006), but these membranes may well be predominantly composed of lipids, because the major protein normally occupying these membranes is nearly or completely missing.

The remaining hypothesis is that a function of wild-type rhodopsin essential for cell survival is not being fulfilled by rhodopsin-GFP. Clues to what that function might be arise from the dysmorphic outer segments observed in mature rods of homozygotes prior to cell death (Figs. 1, 5, and 6). Although rhodopsin-GFP is clearly transported into membranes that are located between the inner segment and the retinal pigmented epithelium (RPE), there are no structures that can be identified as properly formed outer segments. Closely spaced stacks of disk-like membranes (e.g. Fig. 6F) suggest that the mechanisms needed to form closely apposed bilayers with sharply curved edges are still operable in rods lacking free rhodopsin C-termini. However, none of these structures span the entire cell width, and they co-exist with much more disorganized membranes, including what appear to be tubules or spherical vesicles of bilayers. Thus the mechanisms for correctly organizing these stacked membranes appear to be impaired in the absence of a free rhodopsin C-terminus.

The observation of aberrant membrane organization raises the question of whether the disorganization occurs before or after the formation of the outer segments. The developmental program of the photoreceptor layer makes it possible to examine emerging outer segments at the earliest stages of their formation. Prior to the emergence of structures specific to the outer segment, the morphology of the retina from homozygous mouse is indistinguishable from that of the wild type or heterozygous mice; i.e., the other layers of the retina, including the outer nuclear layer containing the photoreceptor nuclei, appear normal. A high density of mitochondria at the distal ends of the rod inner segments is observed in the homozygotes as well as in wild-type retinas, as are the early forms of the connecting cilia (data not shown). However, as soon as disk membranes begin to form, the abnormal organization in homozygote mice becomes readily apparent (Fig. 6F). Although stacks of lamellar membranes resembling distorted disk stacks are present, they are not correctly associated with the connecting cilia. They typically include just a few layers, and are commonly interrupted by vesicles, tubules, and other alternate membrane structures. The abnormal outer membrane structure from the earliest stages of the disease suggests that the lack of normal rhodopsin either prevents proper disk biogenesis, or renders nascent disks highly unstable.

The many mutations in the C-terminus of rhodopsin associated with ADRP point to the functional importance of this region of the protein, and support the idea that the addition of the 25 kDa EGFP moiety could disrupt important functions. The most severe phenotype of this disease arises from a read-through addition of 51 amino acids to the full-length protein (Bessant et al., 1999), a modification not unlike the extension into the EGFP fusion. Mis-sense and deletion mutations at the terminal region of rhodopsin cause ADRP and have been shown both in animal models and in cultured cells to disrupt trafficking of the protein to the outer segment (Deretic et al., 1998; Green, Menz, La Vail, & Flannery, 2000; Sung, Makino, Baylor, & Nathans, 1994; Tam et al., 2000). The C-terminal five amino acids in

rhodopsin have been implicated as the sorting motif regulating the budding of rhodopsin transport carriers from the *trans*-Golgi network (Deretic et al., 2005).

Although rhodopsin's carboxyl terminus is known to play an important role in transport of rhodopsin to outer segments, disruption of that function does not appear to be decisive in the membrane defects observed in rods expressing rhodopsin-EGFP. In heterozygotes there is no detectable difference between the intracellular distributions of rhodopsin and rhodopsin-EGFP, and fluorescent microscopy shows that even in the homozygotes the outer segment area contains rhodopsin-GFP. Rather, the defect appears to revolve around the organization of the disk membranes, a role not previously observed for rhodopsin's carboxyl terminus.

Despite the defects in outer segment membrane formation, there is no gross accumulation of rhodopsin-GFP in the inner segment or synaptic terminal. In fact, only when there are no remaining outer segment-like structures and a single layer of nuclei remains is the majority of rhodopsin-GFP localized to the plasma membrane of the inner segment. The malformation of outer segments in homozygotes could instead direct disruption of the plasma membrane around the rods, whose density of rhodopsin is about half that of the disk membranes (Molday & Molday, 1987), thereby causing a perturbation in ionic homeostasis in rods, leading eventually to apoptosis of the retina.

Defects in other genes important for outer segment biogenesis support the notion that defects in this process can lead to severe disease. One of these is the gene encoding peripherin/rds, a tetraspannin protein localized to the edges of disks and essential for forming tightly curved disk rims. The C214S mutation in peripherin/rds leads to autosomal dominant retinitis pigmentosa (ADRP) in human patients, and has been proposed to result from haploinsufficiency. Mice heterozygous for a null mutation in peripherin/rds (+/*rds*) have defects in outer segment membrane formation that are less severe than observed in homozygotes (Sanyal & Jansen, 1981), and results with mice expressing the C214S peripherin/rds transgene on the null background suggest that the protein level from one wild-type allele is not enough to maintain the OS structure (Stricker, Ding, Quiambao, Fliesler, & Naash, 2005).

Whereas disk membranes are unique to photoreceptors, these primary sensory neurons share with other neurons a reliance for their function on the formation of highly specialized and polarized membrane structures. Now that we have identified the primary defect in the *hrhoG/hrhoG* mice as a failure of proper outer segment membrane biogenesis, these mice can serve as models for further studies of the details of this important process and its disruption in neurodegenerative disease.

Acknowledgments

References

Bessant, D. A., Khaliq, S., Hameed, A., Anwar, K., Payne, A. M., Mehdi, S. Q., et al. (1999). Severe autosomal dominant retinitis pigmentosa caused by a novel rhodopsin mutation (Ter349Glu). *Human Mutation, 13*(1), 83.

Bibb, L. C., Holt, J. K., Tarttelin, E. E., Hodges, M. D., Gregory-Evans, K., Rutherford, A., et al. (2001). Temporal and spatial expression patterns of the CRX transcription factor and its downstream targets. Critical differences during human and mouse eye development. *Human Molecular Genetics, 10*(15), 1571–1579.

Chan, F., Bradley, A., Wensel, T. G., & Wilson, J. H. (2004). Knock-in human rhodopsin-GFP fusions as mouse models for human disease and targets for gene therapy. *Proceedings of the National Academy of Sciences of the United States of America, 101*(24), 9109–9114.

Chen, C. K., Burns, M. E., Spencer, M., Niemi, G. A., Chen, J., Hurley, J. B., et al. (1999). Abnormal photoresponses and light-induced apoptosis in rods lacking rhodopsin kinase. *Proceedings of the National Academy of Sciences of the United States of America, 96*(7), 3718–3722.

Chen, J., Simon, M. I., Matthes, M. T., Yasumura, D., & La Vail, M. M. (1999). Increased susceptibility to light damage in an arrestin knockout mouse model of Oguchi disease (stationary night blindness). *Investigative Ophthalmology and Visual Science, 40*(12), 1978–1982.

Choi, S., Hao, W., Chen, C. K., & Simon, M. I. (2001). Gene expression profiles of light-induced apoptosis in arrestin/rhodopsin kinase-deficient mouse retinas. *Proceedings of the National Academy of Sciences of the United States of America, 98*(23), 13096–13101.

Chuang, J. Z., & Sung, C. H. (1998). The cytoplasmic tail of rhodopsin acts as a novel apical sorting signal in polarized MDCK cells. *Journal of Cell Biology, 142*(5), 1245–1256.

Deretic, D., Schmerl, S., Hargrave, P. A., Arendt, A., & McDowell, J. H. (1998). Regulation of sorting and post-golgi trafficking of rhodopsin by its C-terminal sequence QVS(A)PA. *Proceedings of the National Academy of Sciences of the United States of America, 95*, 10620–10625.

Deretic, D., Williams, A. H., Ransom, N., Morel, V., Hargrave, P. A., & Arendt, A. (2005). Rhodopsin c terminus, the site of mutations causing retinal disease, regulates trafficking by binding to ADP-ribosylation factor 4 (ARF4). *Proceedings of the National Academy of Sciences of the United States of America, 102*(9), 3301–3306.

Fain, G. L., & Lisman, J. E. (1993). Photoreceptor degeneration in vitamin A deprivation and retinitis pigmentosa: the equivalent light hypothesis. *Experimental Eye Research, 57*(3), 335–340.

Fain, G. L., & Lisman, J. E. (1999). Light, Ca2+, and photoreceptor death: new evidence for the equivalent-light hypothesis from arrestin knockout mice. *Investigative Ophthalmology and Visual Science, 40*(12), 2770–2772.

Fujiki, K., Hotta, Y., Murakami, A., Yoshii, M., Hayakawa, M., Nicholas, M. G., et al. (1995). Heterozygous Asn-15-Ser and Gly-174-Ser mutations in the rhodopsin gene found in Japanese retinitis pigmentosa. *Investigative Ophthalmology and Visual Science*(Suppl. S890).

Green, E. S., Menz, M. D., La Vail, M. M., & Flannery, J. G. (2000). Characterization of rhodopsin mis-sorting and constitutive activation in a transgenic rat model of retinitis pigmentosa. *Investigative Ophthalmology and Visual Science, 41*(6), 1546–1553. http://eyegene.meei.harvard.edu/.

Humphries, M. M., Rancourt, D., Farrar, G. J., Kenna, P., Hazel, M., Bush, R. A., et al. (1997). Retinopathy induced in mice by targeted disruption of the rhodopsin gene. *Nature Genetics, 15*, 216–219.

Klein, R. L., Dayton, R. D., Leidenheimer, N. J., Jansen, K., Golde, T. E., & Zweig, R. M. (2006). Efficient neuronal gene transfer with AAV8 leads

to neurotoxic levels of tau or green fluorescent proteins. *Molecular Therapy, 13*(3), 517–527.

Lee, E. S., Burnside, B., & Flannery, J. G. (2006). Characterization of peripherin/rds and rom-1 transport in rod photoreceptors of transgenic and knockout animals. *Investigative Ophthalmology and Visual Science, 47*(5), 2150–2160.

Lisman, J. E., & Fain, G. L. (1995). Support for the equivalent light hypothesis for RP. *Nature Medicine, 1*(12), 1254–1255.

Molday, R. S., & Molday, L. L. (1987). Differences in the protein composition of bovine retinal rod outer segment disk and plasma membranes isolated by a ricin-gold-dextran denisty perturbation method. *Journal of Cell Biology, 105*(6), 2589–2601.

Rosenfeld, P. J., Crowley, G. S., McGee, T. L., Sandberg, M. A., Berson, E. L., & Dryja, T. P. (1992). A null mutation in the rhodopsin gene causes rod photoreveptor dysfunction and autosomal revessive retinitis pigmentosa. *Nature Genetics, 1*, 209–213.

Sanyal, S., & Jansen, H. G. (1981). Absence of receptor outer segments in the retina of rds mutant mice. *Neuroscience Letters, 21*(1), 23–26.

Schuster, A., Weisschuh, N., Jagle, H., Besch, D., Janecke, A. R., Zierler, H., et al. (2005). Novel rhodopsin mutations and genotype–phenotype correlation in patients with autosomal dominant retinitis pigmentosa. *British Journal of Ophthalmology, 89*(10), 1258–1264.

Stricker, H. M., Ding, X. Q., Quiambao, A., Fliesler, S. J., & Naash, M. I. (2005). The cys414–>ser mutation in peripherin/rds causes a loss-of-function phenotype in transgenic mice. *Biochemical Journal, 388*(2), 605–613.

Sung, C. H., Makino, C., Baylor, D., & Nathans, J. (1994). A rhodopsin gene mutation responsible for autosomal dominant retinitis pigmentosa results in a protein that is defective in localization to the photoreceptor outer segment. *Journal of Neuroscience, 14*, 5818–5833.

Tam, B. M., Moritz, O. L., Hurd, L. B., & Papermaster, D. S. (2000). Identification of an outer segment targeting signal in the COOH terminus of rhodopsin using transgenic Xenopus laevis. *Journal of Cell Biology, 151*(7), 1369–1380.

Wilson, J. H., & Wensel, T. G. (2003). The nature of dominant mutations of rhodopsin and implications for gene therapy. *Molecular Neurobiology, 28*(2), 149–158.